Creep behavior of *in situ* dual-scale particles-TiB whisker and TiC particulate-reinforced titanium composites

Z.Y. Ma[a)]
Department of Metallurgical Engineering, University of Missouri, Rolla, Missouri 65409

S.C. Tjong and X.M. Meng
Department of Physics and Materials Science, City University of Hong Kong, 83 Tat Chee Avenue, Kowloon, Hong Kong, Peoples Republic of China

(Received 22 April 2002; accepted 6 June 2002)

A titanium composite reinforced by *in situ* dual-scale particle, high-aspect-ratio TiB whiskers and fine TiC particulates was fabricated by a reactive hot pressing technique from a B_4C–Ti system. The composite was subjected to creep investigations in compression at 873–923 K. This composite exhibited a stress exponent of 4.5–4.6 and a creep activation energy of 298 kJ/mol. By comparison, unreinforced Ti exhibited a stress exponent of 5.2–5.3 and a creep activation energy of 259 kJ/mol. No change in the stress exponent with varying creep rates was observed in both composite and unreinforced Ti under the investigated creep rates. The creep resistance of the composite was more than one order of magnitude higher than that of the unreinforced Ti. The load transfer mechanism accounted for this result. The creep of both composite and unreinforced Ti was controlled by lattice diffusion in the titanium matrix.

I. INTRODUCTION

Recent years have seen an increased interest in developing titanium matrix composites with discontinuous reinforcements for high-temperature structural applications. Among the reinforcements, TiB and TiC are particularly attractive since they are completely compatible with a titanium matrix. In recent years, novel processing techniques, such as exothermic dispersion, rapid solidification processing, combustion-assisted synthesis, and reactive hot pressing (RHP), have been developed in which the reinforcements are grown *in situ* in the titanium matrix.[1–10] Such composites have good interfacial bonding between the *in situ* reinforcement and the titanium matrix, and a crystallographic orientation relationship has been observed between them.[11] Thus, the adverse effect of the surface layer associated with the added reinforcements is avoided. Therefore, the *in situ* titanium matrix composites are expected to exhibit superior mechanical properties.[1,10]

A fundamental knowledge of the mechanisms influencing creep behavior of the titanium matrix composites is required for their use in high-temperature applications. Unfortunately, the creep studies on these composites are limited, and no consistent experimental results and mechanistic explanations have been obtained so far.[12–18] First, the addition of ceramic reinforcements into the titanium matrix generally results in significant creep strengthening.[7,12–18] However, the strengthening mechanisms are not yet well understood, though microstructural strengthening[13,15] and increase in the modulus of composite[12,13] have been suggested as possible strengthening mechanisms. Secondly, a change in the stress exponent from $n = 2.3$ under low creep rates to $n = 7.2$ under high creep rates has been reported by Zhu *et al.*[16] in the TiB_w/Ti–6Al–4V composite. Similar behavior was also observed in TiC_p/Ti–6Al–4V composites.[12,17] A critical creep strain rate of $4 \times 10^{-6} s^{-1}$ to $1 \times 10^{-5} s^{-1}$, at which a change in stress exponent occurs, was revealed for these composites. However, these researchers did not provide any mechanistic explanation for this change.[12,16,17] Thirdly, while Ma *et al.*[18] and Ranganath and Mishra[13] reported that the stress exponent of 4.1–4.9 obtained at 873–923 K in TiB_w/Ti, Ti_2C_p/Ti, and $(TiB_w + Ti_2C_p)$/Ti composites is close to that for the lattice-diffusion-controlled dislocation climb process in α–Ti ($n = 4.3$),[19] high stress exponents of 6–7 were observed at 823 K by Tsang *et al.*[14] and Ranganath and Mishra[13] in TiB_w/Ti, Ti_2C_p/Ti, and $(TiB_w + Ti_2C_p)$/Ti composites.

Different mechanisms have been proposed to explain the exceptionally high stress exponent observed in titanium matrix composites.[13,14] Ranganath and Mishra[13] suggested that the high values of the stress exponent at 823 K were associated with the transition of creep

[a)]Address all correspondence to this author.
e-mail: zong@umr.edu

mechanism from lattice to pipe diffusion, and a kinetic strengthening term involving volume fraction of reinforcement to the constitutive equation of power-law creep was proposed to interpret the results that creep data cannot merge even after compensation for threshold stress. On the other hand, Tsang *et al.*[14] reported that after incorporation of the composite modulus-compensated effective stress into the power-law creep equation, the creep behavior of both unreinforced Ti and composites containing various volume fractions of TiB whiskers can be described by a modified creep equation. It is important to point out that the creep data range measured by these researchers is relatively narrow, covering only 2–3 orders of magnitude of the creep strain rates. Thus, it is difficult to unambiguously elucidate the operative creep mechanism in these titanium matrix composites.

Westwood has proposed a concept of designer microstructures containing hard particle phases for strength, resilient phases for toughness, and whiskers for creep resistance.[1] The titanium matrix composite fabricated from the Ti–B_4C system contains both rodlike TiB whiskers and equiaxed TiC particles. It is expected that the $(TiB_w + TiC_p)/Ti$ composite would exhibit high strength and creep resistance. Indeed, the $(TiB_w + TiC_p)/Ti$ composite exhibited a higher compressive strength than the TiB_w/Ti composite at temperatures ranging from 623 to 923 K.[9] In a previous work, we investigated the creep behavior of the TiB_w/Ti composite.[18] It was shown that the creep resistance of the TiB_w/Ti composite was much higher than that of unreinforced Ti. In this work, the *in situ* $(TiB_w + TiC_p)/Ti$ composite was subjected to compressive creep investigations at 873–923 K, and four orders of magnitude of creep strain rates were measured. This work aims to (i) study the effect of the *in situ* dual-scale hybrid reinforcements, i.e., TiB whisker and TiC particulate on the creep properties of the composites; (ii) verify whether there is a change in stress exponent with varying creep rates in titanium matrix composites; and (iii) elucidate the operative creep mechanism and strengthening mechanism in discontinuously reinforced titanium matrix composites.

II. EXPERIMENTAL

TiB whisker and TiC particulate mixture-reinforced titanium $[(TiB_w + TiC_p)/Ti]$ composite was used in this study. The composite was fabricated from a B_4C–Ti system by the RHP technique.[9,10] In the process, 60-μm Ti powder (98% purity) and 3-μm B_4C powder (98% purity) were initially mixed in a biaxis rotary mixer and subsequently cold compacted. During blending, the ratio of the two powders was properly adjusted so that 12.1 vol% TiB whisker and 2.9 vol% TiC particulate were generated—assuming that all the *in situ* reactions occurred completely. The as-compacted green billets were degassed and then reaction pressed at 1523 K for 0.5 h in a vacuum. Finally, the as-pressed billets were extruded into rods with an extrusion ratio of 18:1 at 1373 K. Unreinforced Ti sample was also fabricated under identical conditions. The resulting composite was subjected to microstructural examination using optical microscopy and transmission electron microscopy (TEM, JEOL 2010, Tokyo, Japan). The thin foils for TEM were prepared by the ion-milling technique.

The as-extruded composite and unreinforced Ti were subjected to constant load compressive creep tests at 873, 898, and 923 K. Cylindrical compression specimens of 5-mm gauge diameter and 5-mm gauge height were machined from the extruded rods with the specimen axis parallel to the extrusion direction. A universal testing machine (Mayes, model ESM 100, United Kingdom) with compression grip was used. The creep strain of the sample was measured using two parallel linear variable displacement transducers (LVDTs) mounted on the ridges provided on the compression grips. The temperature of the sample was monitored using a thermocouple tied to the center of the specimen. The specimen temperature was controlled within ±1 K.

III. RESULTS

Figures 1(a) and 1(b) show the optical micrographs of the 15 vol% $(TiB_w + TiC_p)/Ti$ composite in the directions parallel and vertical to the extrusion direction. The microstructure of the composite is characterized by unidirectional alignment of rodlike reinforcements along the extrusion direction and uniform distribution of fine particulates. Previous x-ray diffraction (XRD) and TEM examinations have verified that the rodlike whiskers were TiB and the fine particulates were TiC.[9] The unidirectional alignment of the TiB whiskers resulted from the hot extrusion process. The TiB whiskers exhibited a diameter of up to 10 μm, and a length of up to 250 μm. Figure 2 shows a TEM micrograph of the $(TiB_w + TiC_p)/Ti$ composite. A clean interface was revealed between the *in situ* reinforcements (TiB whisker and TiC particulate) and titanium matrix. Furthermore, TEM examinations showed the existence of a lot of nanometer TiC particulates and a certain amount of submicrometer diameter TiB whiskers.

Figure 3 shows a typical compressive creep curve for the 15 vol% $(TiB_w + TiC_p)/Ti$ composite at 898 K under an applied stress of 100 MPa. A well-defined steady-state creep stage is evidently visible from this plot. Similar behavior is also observed in unreinforced Ti. Figure 4 shows the variation of steady state creep rate with applied stress for the 15 vol% $(TiB_w + TiC_p)/Ti$ composite. It is noted that the creep data measured for this composite cover four orders of magnitude of creep strain rates

(6.2×10^{-8} to $8.5 \times 10^{-4} s^{-1}$). Clearly, the data at each temperature in Fig. 4 fit into a straight line with slopes equal to the value of the stress exponent n. The observed linearity in this plot indicates that the creep data follow a power-law equation

$$\dot{\epsilon} = \frac{AGbD_o}{kT} \left(\frac{\sigma}{G}\right)^n \exp\left(-\frac{Q}{RT}\right) \quad , \qquad (1)$$

where $\dot{\epsilon}$ is the steady state creep rate, A is a structure dependent parameter, G is the temperature-dependent shear modulus, b is the Burgers vector, D_o is the frequency factor for diffusion, k is the Boltzmann's constant, T is the absolute temperature, σ is the applied stress, n is the stress exponent, Q is the activation energy, and R is the gas constant. The composite exhibited stress exponents of 4.5, 4.6, and 4.6 at 873, 898, and 923 K, respectively. The variation of steady-state creep rate with applied stress for the unreinforced Ti is shown in Fig. 5. Stress exponents of 5.3, 5.3, and 5.2 were observed for the unreinforced Ti at 873, 898, and 923 K, respectively. Figure 6 shows the effect of temperature on the steady-state creep rate of both the $(TiB_w + TiC_p)$/Ti composite

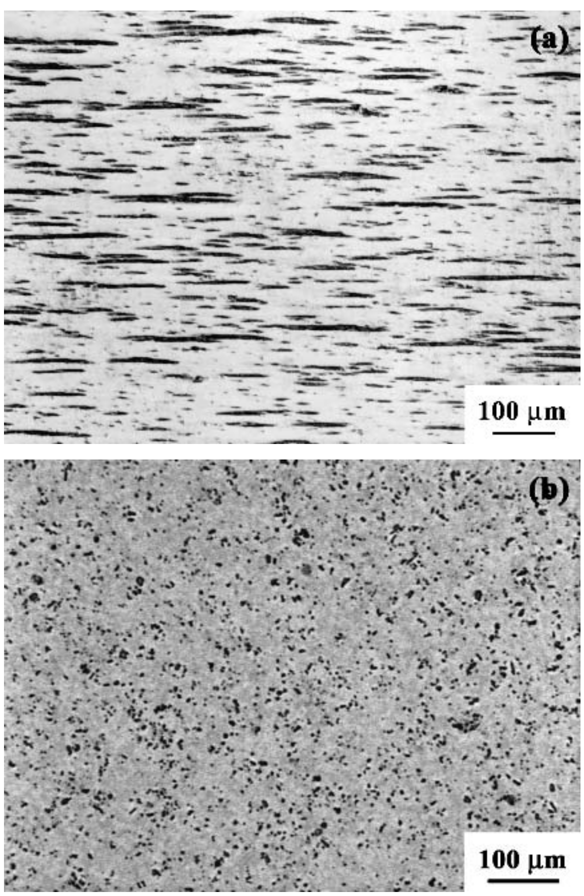

FIG. 1. Optical micrographs showing the distribution of *in situ* reinforcements in 15 vol% $(TiB_w + TiC_p)$/Ti composite: (a) longitudinal direction and (b) traverse direction.

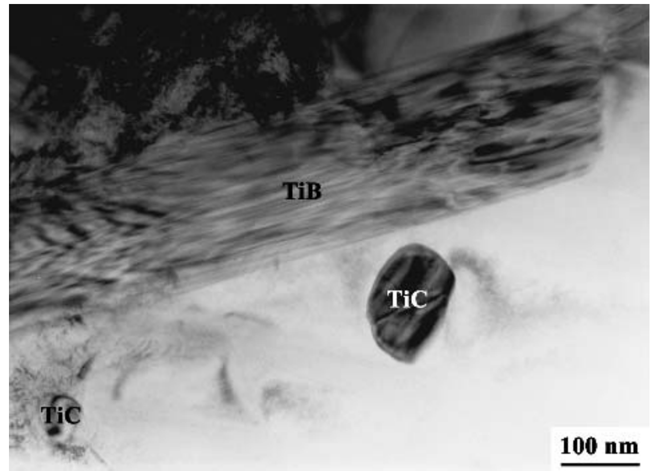

FIG. 2. TEM micrograph showing clean interface between *in situ* reinforcements and titanium matrix in 15 vol% $(TiB_w + TiC_p)$/Ti composite.

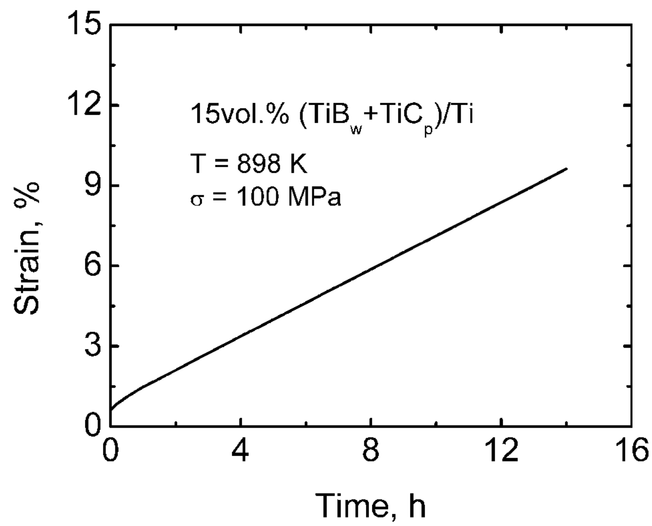

FIG. 3. Typical compressive creep curve for 15 vol% $(TiB_w + TiC_p)$/Ti composite at 898 K under an applied stress of 100 MPa.

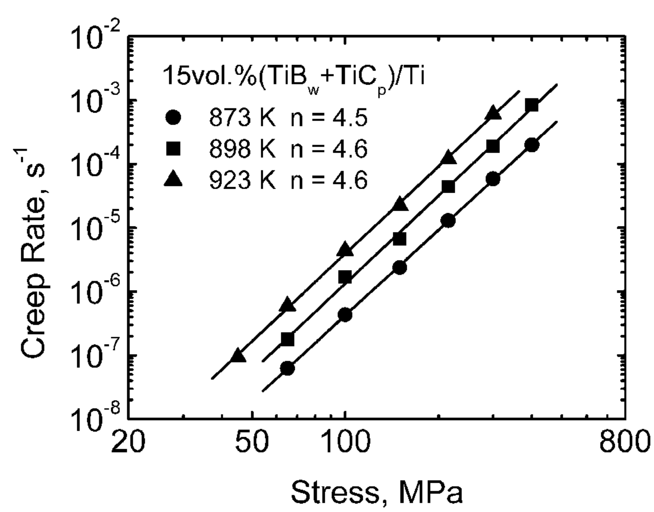

FIG. 4. Variation of steady-state creep rate with applied stress for 15 vol% $(TiB_w + TiC_p)$/Ti composite.

and unreinforced Ti. The activation energy was determined to be 298 kJ/mol for the composite at a constant stress of 215 MPa and 259 kJ/mol for the unreinforced Ti at a constant stress of 65 MPa.

IV. DISCUSSION

Figure 7 shows the comparison between creep rates of 15 vol% ($TiB_w + TiC_p$)/Ti composite and unreinforced Ti at 898 K as a function of applied stress. For comparison, the creep data of 15 vol% TiB_w/Ti composite fabricated under identical conditions[18] is also included in this plot. Clearly, the creep rate of the ($TiB_w + TiC_p$)/Ti composite is more than one order of magnitude lower than that of unreinforced Ti. Similar results were also observed at 873 and 923 K. In previous investigations, other researchers also reported a significant decrease in the creep rate of the titanium matrix composites over the unreinforced titanium matrix.[7,12–16] It is important to note that the creep resistance of the ($TiB_w + TiC_p$)/Ti composite is much higher than that of the TiB_w/Ti composite in the range of investigated temperatures and creep rates. This result is consistent with that of compressive tests at high temperatures of 623–923 K.[9] This indicates that the ($TiB_w + TiC_p$)/Ti composite exhibits superior high-temperature properties over the TiB_w/Ti composite. This is attributed to dual-scale hybrid reinforcements in the ($TiB_w + TiC_p$)/Ti composite, i.e., TiB whiskers and TiC particulates.

Microstructural design in metallic materials for high-temperature applications has received increasing attention in recent years. Westwood proposed that a hybrid microstructure containing both hard particles and whiskers is beneficial for increasing the strength and creep resistance of the materials.[1] Based on analyses of creep data and microstructures of a series of aluminum matrix composites, Mishra suggested an idealized hybrid microstructure for high-temperature aluminum matrix composites; i.e., the composites are reinforced by both nanometer dispersoids and micrometer ceramic particulates.[20] Recently, considering the concept of thermally activated dislocation detachment from dispersoids as a rate-controlling mechanism in dispersion hardened matrices, Rösler and Bäker analyzed theoretically the creep behavior of dual-scale particle strengthened metals containing nanometer size dispersoids and reinforcements with typical dimensions in the micrometer to millimeter range.[21] They revealed that dual-scale particle strengthening can result in very high creep strength levels. Further, they pointed out that rodlike reinforcement with high aspect ratio is effective in strengthening a metal

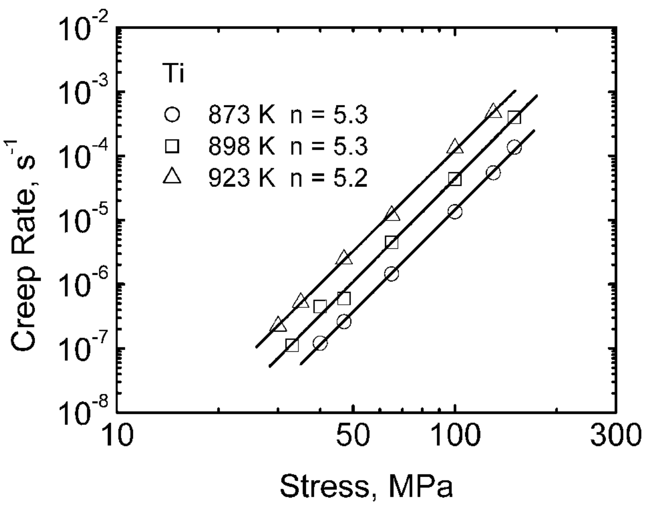

FIG. 5. Variation of steady-state creep rate with applied stress for unreinforced Ti.

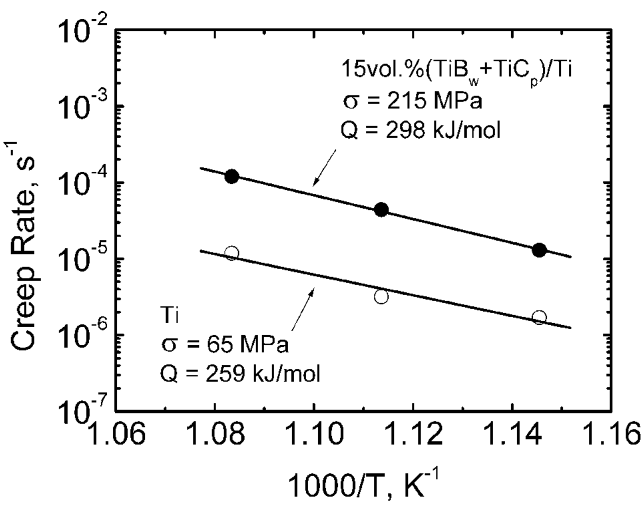

FIG. 6. Effect of temperature on steady-state creep rate for 15 vol% ($TiB_w + TiC_p$)/Ti composite and unreinforced Ti.

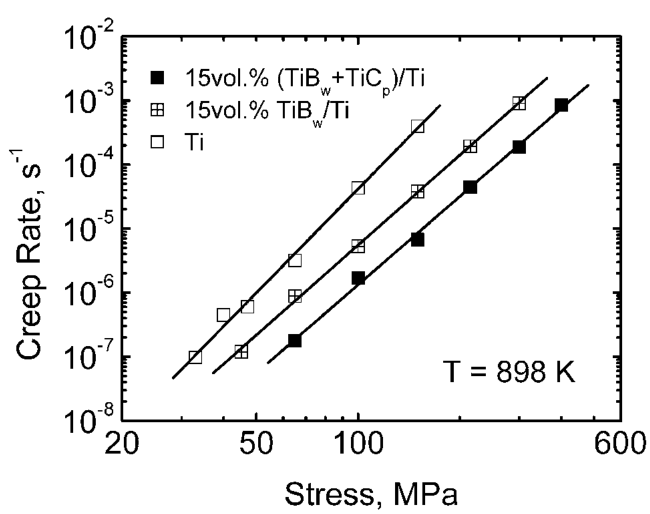

FIG. 7. Comparison between creep rates of 15 vol% ($TiB_w + TiC_p$)/Ti composite, unreinforced Ti, and 15 vol% TiB_w/Ti composite at 898 K as a function of applied stress.

matrix, and a maximum strength is reached when a metallic material is strengthened by the dual-scale particles with a volume fraction ratio of ¾ rodlike reinforcements and ¼ dispersoids. As mentioned above, the $(TiB_w + TiC_p)/Ti$ composite is reinforced by dual-scale particles, i.e., high aspect ratio TiB whiskers and fine equiaxed TiC particulates (Figs. 1 and 2). Clearly, the microstructure in the $(TiB_w + TiC_p)/Ti$ composite is in good agreement with that suggested by Westwood[1] and Rösler and Bäker.[21] Furthermore, the volume fraction ratios of TiB whiskers and TiC particulates in the present $(TiB_w + TiC_p)/Ti$ composite are ⅘ and ⅕, respectively. This ratio is close to that suggested by Rösler and Bäker.[21] Therefore, the dual-scale hybrid reinforcements can account for the higher creep resistance of the $(TiB_w + TiC_p)/Ti$ composite.

From Figs. 4 and 5, it is clear that the present creep data showed no change in the stress exponent with varying creep rates for both 15 vol% $(TiB_w + TiC_p)/Ti$ composite and unreinforced Ti in the range of investigated creep rates (6.2×10^{-8} to 8.5×10^{-4} s^{-1}). Similar results have been observed in the 15 vol% TiBw/Ti composite.[18] The characteristic of constant stress exponent observed in the $(TiB_w + TiC_p)/Ti$ and TiB_w/Ti composites is quite different from that in TiB_w/Ti–6Al–4V and TiC_p/Ti–6Al–4V composites in which a change in stress exponent occurred at a critical creep strain rate of $4 \times 10^{-6} s^{-1}$ to $1 \times 10^{-5} s^{-1}$.[12,16,17] This implies that the composition of the titanium matrix exerts a great influence on the creep behavior of the titanium matrix composites. Further research is needed to elucidate the effect of matrix chemistry on the creep mechanism of the titanium matrix composites.

Figure 4 shows that the 15 vol% $(TiB_w + TiC_p)/Ti$ composite exhibited a stress exponent of 4.5–4.6. These values are very close to that for the lattice-diffusion-controlled dislocation climb process in α-Ti ($n = 4.3$).[19] Similar stress exponent values of 4.1–4.9 were also reported by other researchers in TiB_w/Ti, Ti_2C_p/Ti, and $(TiB_w + Ti_2C_p)/Ti$ composites.[13,14] The unreinforced Ti exhibits a stress exponent of 5.2–5.3. This value is higher than that for α–Ti. Figure 6 shows that the activation energy for creep of unreinforced Ti is 259 kJ/mol, which is close to that for dislocation creep of α–Ti (241 kJ/mol).[19] For the 15 vol% $(TiB_w + TiC_p)/Ti$ composite, the creep activation energy is 298 kJ/mol. This value is slightly larger than that for unreinforced Ti, and close to that (284 kJ/mol) for 10 vol% $(TiB_w + Ti_2C_p)/Ti$ as reported by Ranganath and Mishra.[13] Clearly, the values of the stress exponent and activation energy for creep of the present 15 vol% $(TiB_w + TiC_p)/Ti$ composite suggest that the creep of the composite is associated with the lattice-diffusion-controlled dislocation climb and no threshold stress exists for creep. Thus, the creep data of the composite and unreinforced Ti can be rationalized as $\dot{\epsilon}\, kT/D_L Gb$ versus σ/G (Fig. 8), where $D_L\ [m^2\ s^{-1}] = 1.0 \times 10^{-4} \exp(-241/RT)$, $G\ [MPa] = 4.95 \times 10^4 - 25T$ for α–Ti, $b = 2.89 \times 10^{-10}$ m,[19] and $k = 1.38 \times 10^{-23}$ J mol^{-1} K^{-1}. The creep data of the 15 vol% $(TiB_w + TiC_p)/Ti$ composite merge onto a single straight line with a slope of 4.5. This demonstrates that the creep of the $(TiB_w + TiC_p)/Ti$ composite is controlled by the lattice diffusion in the titanium matrix. However, the normalized creep rate of the composite is still much lower than that of unreinforced Ti, indicating significant creep strengthening of the composite over the unreinforced titanium matrix.

Different mechanisms, e.g., microstructural strengthening[13,15] and increase in the composite modulus,[12,13] have been suggested as possible creep strengthening mechanisms in titanium matrix composites. In discontinuously reinforced aluminum matrix composites, load transfer has been successfully used to explain the creep strengthening by several investigators.[22–24] In this case, part of the external load is transferred to the reinforcement with a corresponding reduction in the level of the effective stress acting on the matrix.[25,26] In the present $(TiB_w + TiC_p)/Ti$ composite, the main reinforcement is TiB whisker with a high aspect ratio. It is well accepted that high-aspect-ratio micrometer reinforcements strengthen the metal matrix by means of load-transfer mechanism.[21] Furthermore, while the fine nanometer TiC particulates retard the creep rate by an attractive interaction between the fine particulates and dislocations, a few large micrometer TiC particulates also contribute to strengthen titanium matrix by load transfer in this titanium matrix composite as in the micrometer particulate reinforced aluminum matrix composites.[22,23] Therefore, it is very likely that the load transfer contributes mainly to the creep strengthening of the $(TiB_w + TiC_p)$/

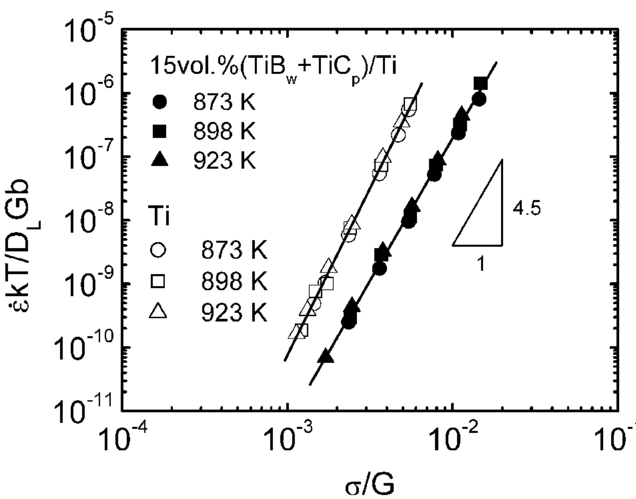

FIG. 8. Variation of normalized creep rate, $\dot{\epsilon}\, kT/D_L Gb$, with modulus-compensated applied stress σ/G for 15 vol% $(TiB_w + TiC_p)/Ti$ composite and unreinforced Ti.

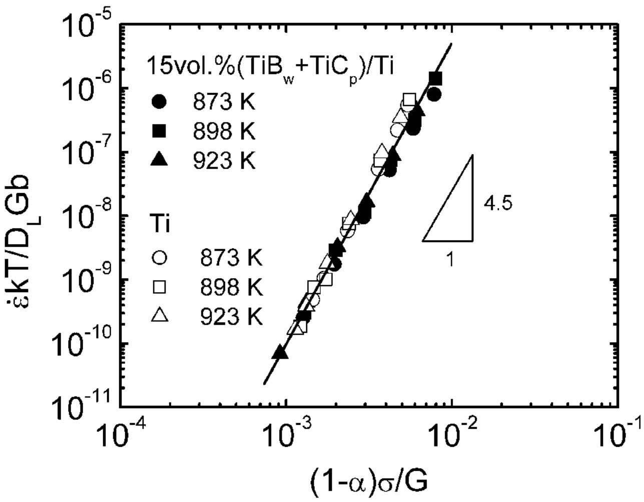

FIG. 9. Variation of normalized creep rate, $\dot{\epsilon}\,\mathrm{k}T/D_L G\mathrm{b}$, with modulus and load transfer coefficient compensated applied stress, $(1-\alpha)\sigma/G$, for 15 vol% ($TiB_w + TiC_p$)/Ti composite and unreinforced Ti.

Ti composite. In this case, a transfer load coefficient α is introduced into the analytical treatment. Thus, the rate-controlling equation is given by

$$\dot{\epsilon} = \frac{AG\mathrm{b}D_o}{\mathrm{k}T}\left[\frac{(1-\alpha)\sigma}{G}\right]^n \exp\left(-\frac{Q}{\mathrm{R}T}\right) \quad . \qquad (2)$$

The value of α lies within a range from 0 (when load transfer is absent) to a maximum value of 1 (when load is transferred completely). For the present 15 vol% ($TiB_w + TiC_p$)/Ti composite, incorporation of the load transfer coefficient α into the analytical treatment results in a α value of 0.46. This means that when 46% of the external load is transferred to the reinforcement the creep strengthening of the 15 vol% ($TiB_w + TiC_p$)/Ti composite can be explained by the load-transfer mechanism. Thus the creep data of both ($TiB_w + TiC_p$)/Ti composite and unreinforced Ti can be described by a united creep equation [Eq. (2)]. Figure 9 shows the creep data normalized by a load-transfer coefficient of 0.46. Clearly, after introducing a load-transfer coefficient, the creep data of both composite and unreinforced Ti merge onto a single straight line with a slope of approximately 4.5. This demonstrates that the load transfer can provide a satisfactory explanation for the creep strengthening of the ($TiB_w + TiC_p$)/Ti composite.

V. CONCLUSIONS

Reactive hot pressing of a Ti–B_4C system resulted in generating a titanium matrix composite reinforced by dual-scale particles–high-aspect ratio TiB whiskers and fine TiC particulates.

15 vol% ($TiB_w + TiC_p$)/Ti composite exhibited a stress exponent of 4.5–4.6 and an activation energy of 298 kJ/mol, whereas unreinforced Ti exhibited a stress exponent of 5.2–5.3 and activation energy of 259 kJ/mol.

There is no change in stress exponent with varying creep strain rate for both 15 vol% ($TiB_w + TiC_p$)/Ti composite and unreinforced Ti in the range of the investigated creep rate (6.2×10^{-8} to 8.4×10^{-4} s^{-1}).

The creep of both 15 vol% ($TiB_w + TiC_p$)/Ti composite and unreinforced Ti is associated with the lattice diffusion-controlled dislocation climb.

The creep resistance of the 15 vol% ($TiB_w + TiC_p$)/Ti composite is more than one order of magnitude higher than that of unreinforced Ti, which can be accounted for by the load-transfer mechanism with a load-transfer coefficient of 0.46.

ACKNOWLEDGMENTS

The authors would like to thank the State Key Laboratory for Fatigue and Fracture of Materials (SKLFFM), Institute of Metal Research, Chinese Academy of Sciences for their support. Thanks are also due to Prof. L. Geng and Mr. Z.Z. Zheng, National Key Laboratory for Precision Hot Processing of Metal, Harbin Institute of Technology, for their assistance with fabrication of the composite.

REFERENCES

1. A.R.C. Westwood, Metall. Trans. **19A,** 749 (1988).
2. S. Ranganath, M. Vijayakumar, and J. Subrahmanyam, Mater. Sci. Eng. **A149,** 253 (1992).
2. Y.X. Lu, D.X. Li, D.H. Ping, J. Bi, and Z.Y. Ma, J. Mater. Sci. Technol. **13,** 41 (1997).
4. S. Ranganath, T. Roy, and R.S. Mishra, Mater. Sci. Technol. **12,** 219 (1996).
5. H.T. Tsang, C.G. Chao, and C.Y. Ma, Scripta Mater. **35,** 1007 (1996).
6. S. Ranganath, J. Mater. Sci. **32,** 1 (1997).
7. W.O. Soboyejo, R.J. Lederich, and S.M.L. Sastry, Acta Metall. Mater. **42,** 2579 (1994).
8. X.N. Zhang, W.J. Lu, D. Zhang, and R.J. Wu, Scripta Mater. **14,** 39 (1999).
9. Z.Y. Ma, S.C. Tjong, and L. Geng, Scripta Mater. **42,** 367 (2000).
10. S.C. Tjong and Z.Y. Ma, Mater. Sci. Eng. Reports **29,** 49 (2000).
11. D.X. Li, D.H. Ping, Y.X. Lu, and H.Q. Ye, Mater. Lett. **16,** 322 (1993).
12. S.J. Zhu, Y.X. Lu, Z.G. Wang, and J. Bi, Mater. Lett. **13,** 199 (1992).
13. S. Ranganath and R.S. Mishra, Acta Mater. **44,** 927 (1996).
14. H.T. Tsang, C.G. Chao, and C.Y. Ma, Scripta Mater. **37,** 1359 (1997).
15. S.J. Zhu, D. Mukherji, W. Chen, Y.X. Lu, Z.G. Wang, and R.P. Wahi, Mater. Sci. Eng. **A256,** 301 (1998).

16. S.J. Zhu, Y.X. Lu, Z.G. Wang, and J. Bi, in *Proc. of Ninth Int. Conf. on Composite Materials (ICCM/9),* edited by A. Miravete (University of Zaragona and Woodhead Publishing Limited, Spain, 1993), Vol. 1, p. 594.
17. J.H. Zhu, P.K. Liaw, J.M. Corum, and H.E. McCoy, Jr., Metall. Mater. Trans. **30,** 1569 (1999).
18. Z.Y. Ma, S.C. Tjong, and S.X. Li, Metall. Mater. Trans. **32A,** 1019 (2001).
19. G. Malakondaiah and P.R. Rao, Acta Metall. **29,** 1263 (1981).
20. R.S. Mishra, JOM **51,** 65 (1999).
21. J. Rösler and M. Bäker, Acta Mater. **48,** 3553 (2000).
22. K.T. Park and F.A. Mohamed, Metall. Mater. Trans. **26A,** 3119 (1995).
23. Y. Li and T.G. Langdon, Metall. Mater. Trans. **29A,** 2523 (1998).
24. L.M. Peng, S.J. Zhu, Z.Y. Ma, F.G. Wang, H.R. Chen, and D.O. Northwood, Mater. Sci. Eng. **A256,** 63 (1999).
25. A. Kelly and K.N. Street, Proc. R. Soc. (London) **328A,** 267 (1972).
26. A. Kelly and K.N. Street, Proc. R. Soc. (London), **328A,** 283 (1972).